Journal of Alloys and Compounds 503 (2010) 340–344

Contents lists available at ScienceDirect

Journal of Alloys and Compounds

journal homepage: www.elsevier.com/locate/jallcom

Synthesis, ^{13}C NMR-MAS, AC conductivity and structural characterization of $[C_7H_{12}N_2]ZnCl_4$

Adel Jarboui*, Bassem Louati, Faouzi Hlel, Kamel Guidara

Laboratoire de l'état solide, Faculté des Sciences de Sfax, Sfax 3018, Tunisia

ARTICLE INFO

Article history:
Received 21 March 2009
Received in revised form
15 September 2009
Accepted 16 September 2009
Available online 23 September 2009

Keywords:
2,4-Diammonium toluene tetrachlorozincate (II)
Crystal structure
^{13}C CP-MAS-NMR spectroscopy
Electrical properties

ABSTRACT

Synthesis, crystal structure, ^{13}C CP-MAS-NMR analysis and impedance spectroscopy study are reported for a new organic–inorganic hybrid salt, $[C_7H_{12}N_2][ZnCl_4]$, consisting of one 2,4-diammonium toluene cation and one $[ZnCl_4]^{2-}$ anion. The Zn atom is in a slightly distorted tetrahedra coordination environment. The structure can be described by the alternation of ionic and organic layers. The cohesion of the material is assured by strong charge-assisted N–H···Cl interactions established between ammonium groups and discrete $[ZnCl_4]^{2-}$ tetrahedra. Solid state ^{13}C CP-MAS-NMR spectra show seven isotropic resonances, confirming the existence of seven non-equivalent carbon atoms which are consistent with the solid state structure determined by X-ray diffraction.

Impedance spectroscopy study, reported for single crystal and powder samples, reveals that the conduction in the material is due to a hopping process along the [1 0 0] direction.

1. Introduction

There is an increasing interest today in open-framework materials due to the numerous high-performance properties that these materials may present. One can find two main classes of open-framework materials. The first corresponds to inorganic compounds in which MO_6 octahedra and/or MO_4 tetrahedra are isolated or share edges or apexes to form 3D frameworks which contain tunnels and/or cavities where ions and/or solvent molecules can be intercalated [1]. The second class corresponds to layered compounds such as smectite clays [2], layered hydroxyl salts [3] and layered double hydroxides [4]. Recently, attention has been drawn to a novel class of open-framework materials namely organic–inorganic hybrid materials. These systems are found to have the advantage in many fields of applications that they combine both inorganic and organic characters [5,6]. Inorganic materials offer the potential for a wide range of electronic properties (enabling the design of insulators, semiconductors, and metals), magnetic and dielectric transitions, substantial mechanical hardness, and thermal stability. Organic molecules, on the other hand, can provide high fluorescence efficiency, large polarizability, plastic mechanical properties, ease of processing, and structural diversity [7,8]. Moreover, the non-covalent interactions, usually observed in hybrid materials, are some of the most powerful forces to organize structural units in both natural and artificial systems, and they have important effects on the organization and properties of many materials in areas such as biology, crystal engineering and material science [9–13]. The hybrid materials encompass organic–inorganic composites that alternate chemically and electronically at the molecular level. All these properties are related to the structural changes of these compounds depending on the effects of different factors such as temperature and composition. In this context we report the synthesis, the crystal structure, ^{13}C NMR-MAS and electrical properties of the 2,4-diammonium toluene tetrachlorozincate (II) compound.

2. Experimental

0.37 g (3 mmol) of $C_7H_{10}N_2$ (ALDRICH, purity: 97%) and 0.41 g (3 mmol) of $ZnCl_2$ (ALDRICH, purity: 98%) were dissolved in 20 ml of HCl (2 M) aqueous solution. The obtained solution was kept at room temperature. After three days, prismatic red-brown crystals appeared (yield: 0.93 g, 93%).

A single crystal (0.52 mm × 0.43 mm × 0.26 mm) was selected by optical examination. Crystallographic measurements were made at room temperature (graphite monochromated Mo K_α radiation, 0.71073 Å) using a Stoe Image Plate Diffraction System and a Siemens SMART CCD area-detector diffractometer. An empirical absorption corrections using SADABS [14] were applied. The structure was solved by Patterson methods and refined in the anisotropic approximation using SHELXS-86 [15] and SHELXL-97 [16]. The main crystal data, the parameters used for intensity data collection and the reliability factor are summarized in Table 1. The obtained solution permits us to localize the positions of zinc and chlorine atoms. Positions of N and all carbon atoms were located after subsequent Fourier series analysis. Hydrogen atoms of the methyl ramification were placed in calculated positions. The other H atoms were successively located in a different

* Corresponding author.
E-mail addresses: adeljarboui@yahoo.fr (A. Jarboui), bassem-louati@yahoo.fr (B. Louati), faouzihlel@yahoo.fr (F. Hlel), kamelguidara@yahoo.fr (K. Guidara).

0925-8388/$ – see front matter © 2010 Published by Elsevier B.V.
doi:10.1016/j.jallcom.2009.09.072

Table 1
Summary of crystal data, intensity measurements and refinement parameters for $[C_7H_{12}N_2][ZnCl_4]$.

Formula: $[C_7H_{12}N_2][ZnCl_4]$	Fw = 332.36 g mol^{-1}
Color/shape	Red-brown/prismatic
Crystal dimensions	0.52 mm × 0.43 mm × 0.26 mm
Crystal system	Monoclinic
Space group	$P2_1/c$ (No. 14)
a = 6.9734(1) Å, b = 9.8088 (3) Å, c = 18.4663(4) Å, β = 93.256(1)	V = 1261.07(5) Å^3, Z = 4, μ = 2.76 mm^{-1}
Temperature (K)	293(2)
Radiation, λ (Å), monochromator	Mo K_α, 0.71069, graphite
Scan angle (°)	θ–2θ
2θ range (°)	2.2–36.8
Range of h, k, l	−11 → 11, −16 → 8, −26 → 30
Reflections collected/unique	11831/5943 (R_{int} = 0.024)
Observed reflections [Fo > 2σ(Fo)]	4739
Absorption correction	Multi-scan (SADABS)
T_{min}, T_{max}	0.542, 0.823
Structure resolution	Paterson methods: SHELXS-86
Structure refinement with	SHELXL-97
Refinement	F^2 full matrix
Refined parameters	164
Goodness of fit	1.008
Final R and Rw	0.028, 0.085
Final R and Rw (for all data)	0.043, 0.114
Largest feature diff. map	0.719, −0.166e$^-$/Å^3
$w = 1/[\sigma\ (Fo)^2 + (0.0677P)^2 + 0P$	$P = [Fo^2 + 2\ Fc^2]/3$

Table 2
Main distances (Å) and bond angles (°) in the $[C_7H_{12}N_2][ZnCl_4]$ (e.s.d. are given in parentheses).

Distances (Å)		Angles (°)	
$ZnCl_4$			
Zn–Cl1	2.264(1)	Cl1–Zn–Cl2	106.5(2)
Zn–Cl2	2.284(1)	Cl1–Zn–Cl3	106.7(2)
Zn–Cl3	2.279(1)	Cl1–Zn–Cl4	112.4(2)
Zn–Cl4	2.237(1)	Cl2–Zn–Cl3	110.5(2)
		Cl2–Zn–Cl4	107.4(2)
		Cl3–Zn–Cl4	113.1(2)
$C_7H_{12}N_2^+$			
C5–C4	1.375(2)	C4–C5–C6	119.2(2)
C5–C6	1.375(3)	C5–C6–C1	122.1(2)
C6–C1	1.392(2)	C3–C2–C1	123.0(1)
C2–C3	1.384(2)	C3–C2–N1	117.9(1)
C2–C1	1.392(2)	C1–C2–N1	119.1(1)
C2–N1	1.467(2)	C4–C3–C2	117.7(1)
C3–C4	1.380(2)	C5–C4–C3	121.6(2)
C4–N2	1.460(2)	C5–C4–N2	119.8(1)
C1–C	1.498(2)	C3–C4–N2	118.6(1)
		C2–C1–C6	116.5(2)
		C2–C1–C	122.3(2)
		C6–C1–C	121.2(2)

Fourier maps. Main geometrical features, bond distances and angles are reported in Tables 2 and 3.

The NMR experiments were performed at room temperature on a Bruker MSL 300 spectrometer operating at 75.48 MHz for ^{13}C. The powdered sample was packed in a 4 mm diameter rotor and allowed to rotate at speeds up to 10 kHz in a Doty MAS probehead. During the whole acquisition time, the spinning rate of the rotor was locked to the required value thanks to the Bruker pneumatic unit which controls both bearing and drive inlet nitrogen pressures. The spectra were acquired by use of cross-polarization for proton with 5 ms contact time. All chemical shifts (δ) are given with respect to tetramethylsilane, according to the IUPAC convention, i.e. shielding corresponds to negative values. Spectrum simulation was performed by using Bruker WINFIT software [17].

The electrical measurements were performed using a two-electrode configuration on polycrystalline and single crystal samples. The polycrystalline sample was pressed into pellets of 8 mm diameter and 1.1 mm thickness using 3t/cm^2 uniaxial pressure. Several crystallization tests allowed us to obtain crystals with suitable dimensions to undertake an electrical study. The used crystal has a 20 mm^2 of surface and 2 mm of thickness. We note that the great crystal surfaces are perpendicular to a direction. Indeed, in the case of the single crystal, the measurements were performed along [1 0 0] direction. Electrical impedances were measured in a frequency ranging from 200 Hz to 5 MHz with the TEGAM 3550 ALF automatic bridge monitored by a microcomputer between 408 and 468 K.

Table 3
Main interatomic distances (Å) and bond angles (°) involved in hydrogen bonds (e.s.d. are given in parentheses).

N–H···Cl	N–H	H···Cl	N···Cl	N–H···Cl
N1–HN11···Cl2	0.95(3)	2.33(2)	3.26(3)	175(2)
N1–HN12···Cl2	0.89(4)	2.32(4)	3.21(4)	169(3)
N1–HN13···Cl3	0.84(3)	2.48(2)	3.33(3)	174(3)
N2–HN21···Cl4	0.96(3)	2.20(3)	3.15(4)	168(2)
N2–HN22···Cl1	0.95(6)	2.43(2)	3.22(2)	140(3)
N2–HN23···Cl3	0.95(5)	2.44(3)	3.31(3)	152(2)

3. Results and discussion

3.1. Structure description

The asymmetric unit of the title compound is made up of one $ZnCl_4^{2-}$ anion and a single 2,4-diammonium toluene dication. A view of the asymmetric unit of the structure drawing with 50% probability thermal ellipsoids is depicted in Fig. 1. The crystal structure consists of alternating layers of organic and inorganic corrugated sheets stacked along [1 0 0] direction, Fig. 2. Organic and inorganic layers are interconnected through five N–H···Cl hydrogen bonds and one bifurcated hydrogen bonding established by HN22 atom, Fig. 3. Each organic cation is linked to four $ZnCl_4^{2-}$ tetrahedra. The corresponding N···Cl distances vary between 3.15(4) and 3.31(3) Å, which can be considered relatively weak [18]. In the inorganic layers, there are no π–π interaction between identical parallel 2,4-diammonium toluene cations, with face-to-face distances of 4.452(3) Å which is longer than values observed in similar compounds [19].

The zinc atom is tetrahedrally coordinated by chlorine atoms, with Zn–Cl distances ranging from 2.237(5) to 2.284(4) Å and Cl–Zn–Cl angles varying from 106.5(2)° to 113.1(2)°. Those values show a slight distortion of the $ZnCl_4^{2-}$ tetrahedra. These results are similar to the data known for the tetrachlorozincate anion [19–21].

The organic molecule exhibits a regular spatial configuration with normal distances C–C, C–N and angles C–C–C, C–C–N. The main value of the C–C length of the C_6-ring is 1.383(2) Å, which is between single and double bonds and agrees with that observed in the C_6-ring of benzene derivatives [22]. All the carbon atoms of the C_6-ring are coplanar with an average deviation of 0.004 Å. Furthermore, the distances C(1)–C, C(2)–N(1) and C(4)–N(2)

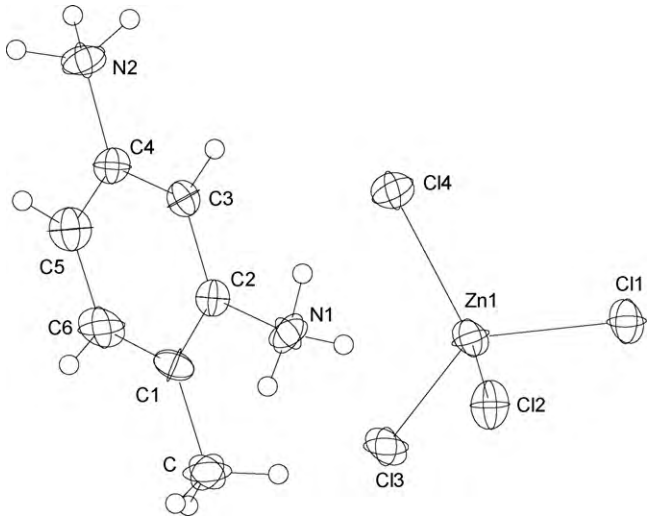

Fig. 1. Asymmetric unit of $[C_7H_{12}N_2][ZnCl_4]$, with atom labels and 50% probability displacement ellipsoids for non-H atoms.

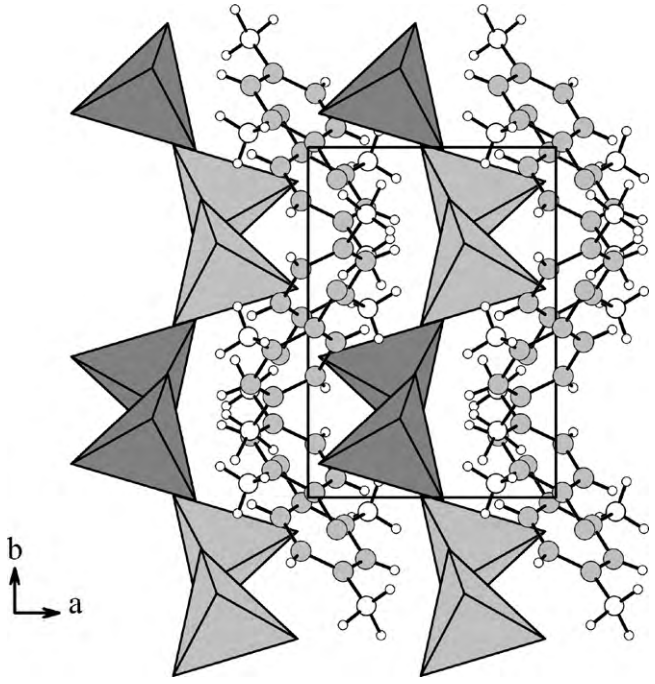

Fig. 2. Crystal structure of the title compound, viewed down the *c*-axis, showing the layer sequence. The big empty circles represent nitrogen atoms, light grey circles represent carbon and small empty circles represent H atoms. $ZnCl_4$ units are represented by tetrahedra.

[1.498(2), 1.467(2) and 1.460(2) Å], clearly indicate three single bonds.

3.2. NMR spectroscopy

The isotropic band of ^{13}C CP-MAS-NMR spectrum of the crystalline 2,4-diammonium toluene tetrachlorozincate (II) sample rotating at magic angle with frequency 10 kHz is given in Fig. 4. Spinning the sample at 8 kHz speed allowed us to assign the isotropic band. Simulation of the isotropic band permits to identify seven peaks (Table 4). The presence of seven resonances corresponds to the seven carbon atoms of the organic cation. This result proves the presence of only one organic cation in the asymmetric unit of the compound. The signal at 19.7 ppm corresponds to the methyl carbon atom. The other resonances at higher chemical shift correspond to the aromatic carbon atoms of the phenyl

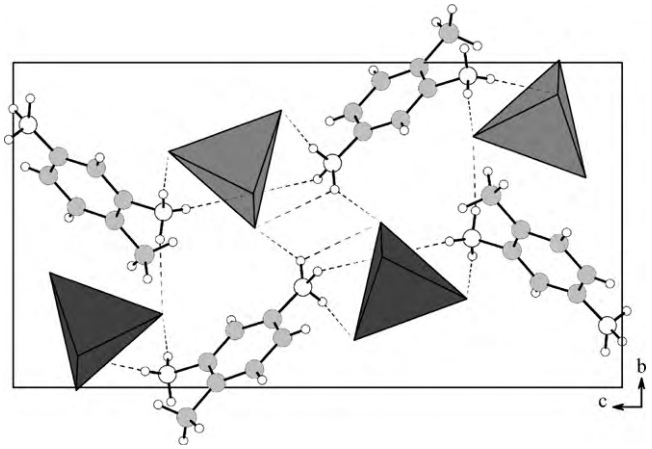

Fig. 3. The packing of $[C_7H_{12}N_2][ZnCl_4]$, viewed down the *a*-axis, showing anions and cations connected by N–H···Cl hydrogen bonds (dashed lines).

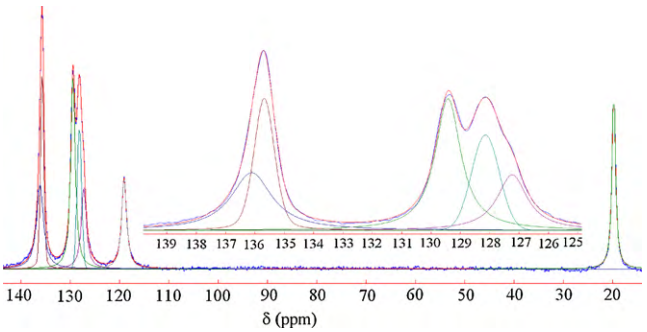

Fig. 4. Plots of experimental and fitted curves of the isotropic band of the ^{13}C CP-MAS-NMR spectrum of the crystalline 2,4-diammonium toluene tetrachlorozincate (II) sample rotating at magic angles with a frequency of 10 kHz. To show all fitted resonances, peaks observed at higher frequency are zoomed in inserted plot.

ring. The more shielded chemical shift values, 136.1 and 135.7 ppm, can be attributed to carbon atoms, C(2) and C(4) of the C_6-ring, linked to the electronegative atoms N(1) and N(2). The chemical shift values were commonly observed in aniline derivative [23].

3.3. Electrical properties

Fig. 5 shows the plot of imaginary part (Z'') versus real part (Z') of complex impedance taken over the frequency range 200 Hz to 5 MHz at different temperatures 420 K ≤ *T* ≤ 468 K. All the semicircles of the polycrystalline compound exhibit some depression instead of a semicircle centered on the real axis. Such behavior is indicative of non-Debye type of relaxation and it also manifests that there is a distribution of relaxation times instead of a single relaxation times in the material [24].

The bulk ohmic resistance relative to each experimental temperature is deduced from complex impedance diagrams, it is the interception Z_0 on the real axis of the zero phase angle of extrapolation in the lower frequency curve. The conductivity σ is obtained from Z_0 by means of the relation: $\sigma = e/Z_0S$, where *e* and *S* represents the thickness and the area of the sample, respectively. The temperature dependence of the conductivity in the studied temperature range is given in Fig. 6 for polycrystalline and single crystal as a plot of $\ln(\sigma T)$ versus reciprocal temperature. Arrhenius-type behavior is clearly exhibited.

A linear fit to $\sigma T = A\exp(-E_\sigma/k_\beta T)$, where *A* is the pre-exponential factor, E_σ is the apparent activation energy for the mobile ions, k_β is the Boltzmann constant and *T* is the absolute temperature, is shown. Electrical data relative to these materials are listed in Table 5.

The electrical properties reported in Table 5 can be compared. Independently of the polycrystalline or single crystal, the $[C_7H_{12}N_2][ZnCl_4]$ compound is characterized by a higher activation energy E_σ (2.1 ± 0.1) eV. However, compared with the polycrystalline compound, the single crystal $[C_7H_{12}N_2][ZnCl_4]$ is

Table 4
^{13}C CP-MAS-NMR peaks characteristics observed in the isotropic band for the spectrum recorded at 10 kHz of the compound $[C_7H_{12}N_2][ZnCl_4]$ with e.s.d. equal to 0.1 ppm.

Peaks	δ_{iso} (ppm)	FWHM (ppm)
1	19.7	0.86
2	119.1	1.21
3	127.2	1.24
4	128.2	1.12
5	129.4	1.06
6	135.7	0.83
7	136.1	1.68

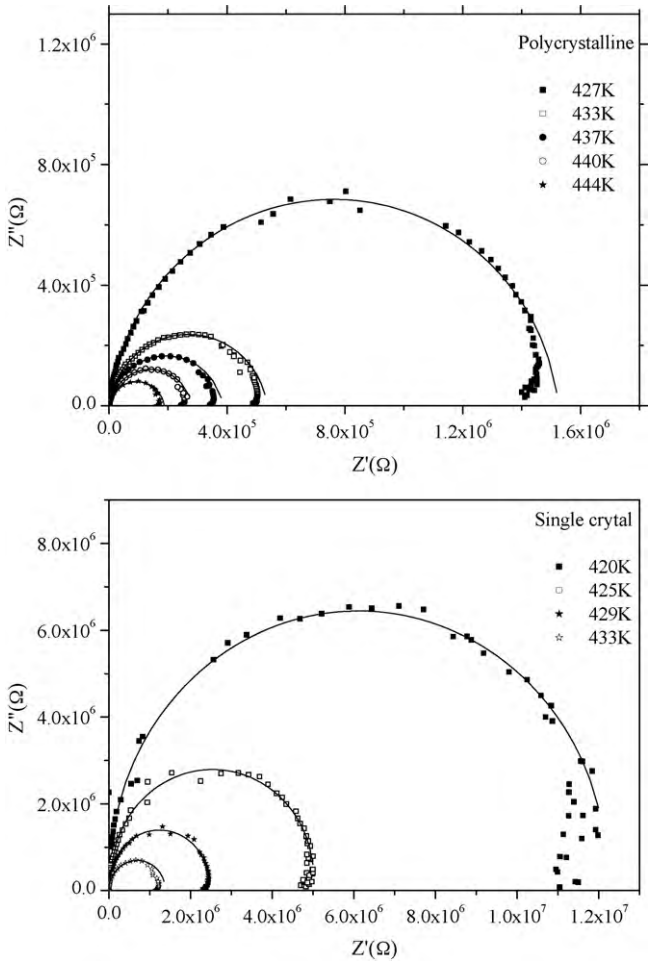

Fig. 5. Complex impedance plots of $Z''(\Omega)$ versus $Z'(\Omega)$ at various temperatures for $[C_7H_{12}N_2][ZnCl_4]$ compound.

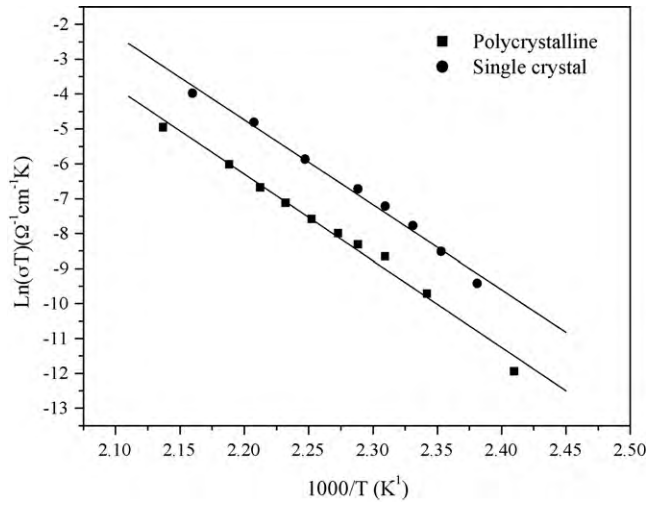

Fig. 6. Temperature dependence of $\ln(\sigma T)$ versus reciprocal temperature for $[C_7H_{12}N_2][ZnCl_4]$.

Table 5
Electrical parameters of polycrystalline and single crystal $[C_7H_{12}N_2][ZnCl_4]$.

	Polycrystalline	Single crystal
σ (Ω^{-1} cm^{-1}) (T = 400 K)	7.07×10^{-7}	3.36×10^{-6}
E_σ (±0.1 eV)	2.1	2.1

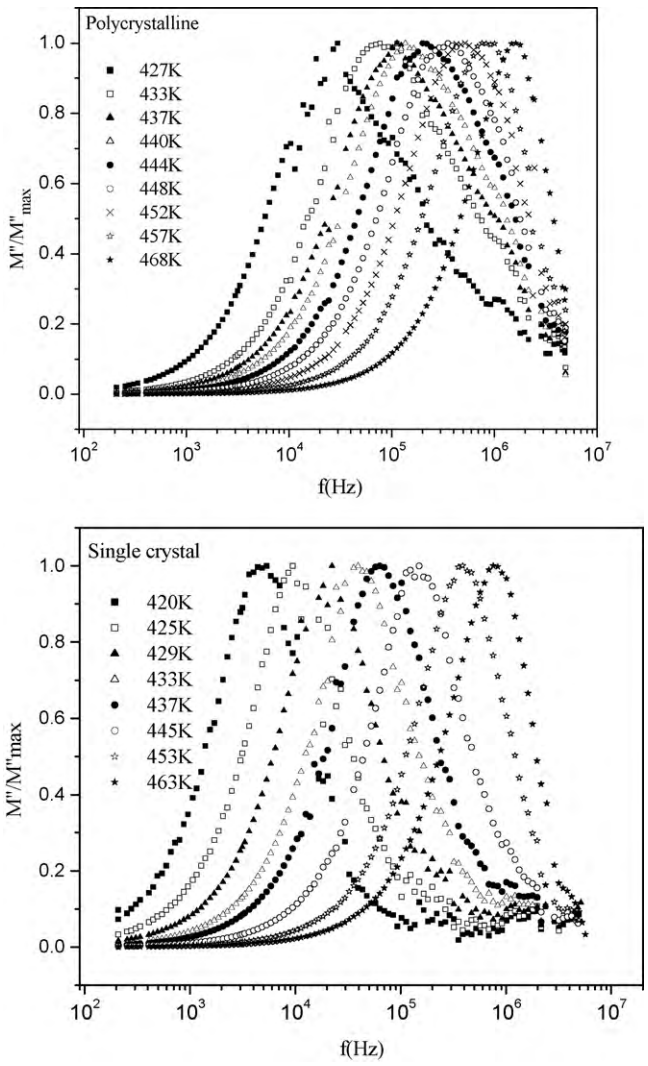

Fig. 7. Normalized modulus M''/M''_{max} at various temperatures for polycrystalline and single crystal $[C_7H_{12}N_2][ZnCl_4]$.

characterized by a higher value of σ_0. At 400 K, the conductivity jumps about 5 times. This increase suggests that most of transport properties are probably due to displacements of charge carriers along [1 0 0] direction which corresponds to the direction of the stacking of the corrugated organic and inorganic sheets.

An analysis of the ion conductivity relaxation process in polycrystalline and single crystal have been undertaken in the complex modulus M^* formalism. This formalism ($M^* = 1/\varepsilon^* = j\omega C_0 Z^*$, C_0 is the vacuum capacitance of the cell) is useful in determining the charge carriers parameters such as the ion hopping rate and the conductivity relaxation time [25,26].

Some spectra of normalized modulus, M'/M''_{max} relative to various temperatures are reported in (Fig. 7) for polycrystalline and single crystal samples. The frequency range where the peak occurs is indicative of the transition from short-range to long-range mobility at decreasing frequency and is defined by the condition $\omega\tau_f = 1$, where τ_f is the most probable ion relaxation time [27]. When temperature increases, modulus peak maxima shifts to higher frequencies (Fig. 7).

Fig. 8 gives the temperature dependence of the f_p ($f_p = 1/2\pi\tau_f$) frequency relative to M''/M''_{max}. An Arrhenius-type law is shown and the activation energies are (1.9 ± 0.1) and (2.0 ± 0.1) eV for the single crystal and polycrystalline compounds, respectively.

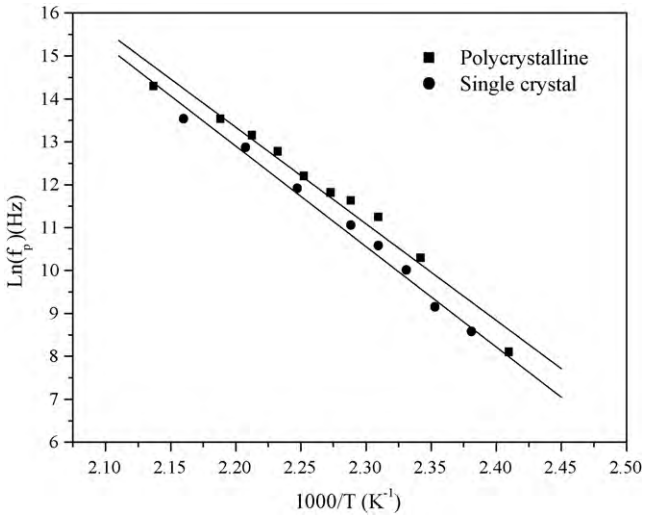

Fig. 8. Inverse temperature dependence of $\ln(f_p)$ versus reciprocal temperature for polycrystalline and single crystal.

The activation energies issued from the impedance E_σ and modulus E_f spectra are close enough to suggest that the ion transport in polycrystalline and single crystal are probably due to a hopping mechanism [28].

4. Conclusions

Crystals of a hybrid material, $[C_7H_{12}N_2][ZnCl_4]$, have been prepared by slow evaporation of aqueous solution HCl (2 M), $C_7H_{10}N_2$ and $ZnCl_2$ at room temperature. The atomic arrangement is characterized by infinite corrugated layers of inorganic anions alternating with organic sheets stacked along a direction. In addition, the two layers spreading in this network are themselves interconnected by weak H-bonds established between NH_3 groups of organic cations and chlorine atoms $ZnCl_4$ tetrahedron.

^{13}C CP-MAS-NMR spectra evidence seven different isotropic peaks relative to carbon atoms of one organic cation in the structure.

The electrical properties of $[C_7H_{12}N_2][ZnCl_4]$ material were studied as a function of frequency and temperature ranges (200 Hz to 5 MHz) and (420–468 K), respectively.

Independently of the single crystal or polycrystalline state, $[C_7H_{12}N_2][ZnCl_4]$, is characterized by the same activation energy E_σ (2.1 ± 0.1) eV. However, the conductivity of the single crystal (T = 400 K) is about 5 times more important suggesting that the transport is probably in [1 0 0] direction corresponding to the direction of stacking of the corrugated organic and inorganic sheets.

The analysis of the temperature variation of M'' peak indicates that the observed relaxation process is thermally activated. The near value of activation energies obtained from the relaxation times and conductivity data confirms that the transport is through ion hopping mechanism in the investigated material.

Supplementary materials

CCDC 688770 contains the supplementary crystallographic data for this paper. This data can be obtained free of charge via http://www.ccdc.cam.ac.uk/conts/retrieving.html, or from the Cambridge Crystallographic Data Centre, 12 Union Rood, Cambridge CB2 1EZ, UK (Fax: (international) +44 1223/336 033; e-mail: deposit@ccdc.cam.ac.uk).

References

[1] S. Litty, Y. Piffard, A.K. Shukla, F. Taulelle, J. Gopalakrishnan, J. Mater. Chem. 13 (2003) 1797.
[2] T. Pinnavaia, J. Sci. 22 (1983) 365.
[3] F. Cavani, F. Trifiro, A. Vaccari, Catal. Today 11 (1991) 173.
[4] L. Poul, N. Jouini, F. Fievet, Chem. Mater. 12 (2000) 3123.
[5] A.M. Fonseca, C.J.R. Silva, N. Nunes, I.C. Neves, J. Alloys Compd. 454 (2008) 72.
[6] Z. Peng, X. Xing, X. Chen, J. Alloys Compd. 425 (2006) 323.
[7] D.B. Mitzi, K. Chondroudis, C.R. Kagan, IBM J. Res. Dev. 45 (2001) 29.
[8] I. Chaabane, F. Hlel, K. Guidara, J. Alloys Compd. 461 (2008) 495.
[9] B. Gawel, W. Lasocha, M. Zieba, J. Alloys Compd. 442 (2007) 77.
[10] K.M. Guckian, B.A. Schweitzer, R.X.F. Ren, C.J. Sheils, D.C. Tahmassebi, E.T. Kool, J. Am. Chem. Soc. 122 (2000) 2213.
[11] S.Y. Mao, Y. Xie, Z.X. Xie, L.S. Zheng, J. Alloys Compd. 456 (2008) 534.
[12] A.L. Gillon, A.G. Orpen, J. Starbuck, X.M. Wang, Y. Rodriguez-Martin, C. Ruiz-Perez, Chem. Commun. (1999) 2287.
[13] L. Brammer, J.C. Mareque Rivas, R. Atencio, S. Fang, F.C. Pigge, J. Chem. Soc., Dalton Trans. (2000) 3855.
[14] G.M. Sheldrick, SADABS, University of Göttingen, Germany, 2004.
[15] G.M. Sheldrick, SHELXS-86, Program for Crystal Structure Solution, University of Göttingen, Germany, 1986.
[16] G.M. Sheldrick, SHELXL-97, Program for Crystal Structure Refinement, University of Göttingen, Germany, 1997.
[17] D. Massiot, H. Theile, A. Germany, Bruker Report, vol. 43, 1994, p. 140.
[18] I.D. Brown, Acta Crystallogr. A32 (1976) 24.
[19] Z.-M. Jin, N. Shun, Y.-P. Lü, M.-L. Hu, L. Shen, Acta Crystallogr. C61 (2005) m43.
[20] F. Hlel, A. Rheim, T. Guerfel, K. Guidara, Z. Naturforsch. 61B (2006) 1002.
[21] N. Guo, J. Yi, Y. Chen, S. Liao, Z. Fu, Acta Crystallogr. E63 (2007) m2571.
[22] F. Hlel, R. Thouvenot, L. Smiri, Phys. Stat. Sol. (B) 242 (2005) 1243.
[23] H.C. Galka, L.H. Gade, Inorg. Chim. Acta 357 (2004) 1725.
[24] S. Sen, R.N.P. Choudhary, P. Pramanik, Physica B 387 (2007) 56.
[25] D.P. Almond, A.R. West, Solid State Ionics 11 (1983) 57.
[26] B.V.R. Chowdari, K. Radhakrishnan, J. Non-Cryst. Solids 110 (1989) 101.
[27] H.K. Patel, S.W. Martin, Phys. Rev. B45 (1992) 10292.
[28] J.M. Réau, S. Rossignol, B. Tanguy, J.M. Rojo, P. Herrero, R.M. Rojas, J. Sanz, Solid State Ionics 74 (1994) 65.